Heat and Mass Transfer (2019) 55:445–465
https://doi.org/10.1007/s00231-018-2435-y

ORIGINAL

Comparative investigation and multi objective design optimization of R744/R717, R744/R134a and R744/R1234yf cascade rerfigeration systems

Mert Sinan Turgut[1] · Oguz Emrah Turgut[1]

Received: 7 September 2017 / Accepted: 24 July 2018 / Published online: 28 July 2018

Abstract

This study aims to make a comparative investigation on performance analysis of cascade refrigeration systems using R744/R717, R744/R134a, and R744/R1234yf refrigerant pairs. Artificial Cooperative Search methaheuristic algorithm is put into practice to obtain the optimal values of eight design parameters including Condenser and evaporator temperature, R744 condensing temperature, temperature difference in the cascade condenser, and amount of subcooling and superheating at the bottom and the top of the cascade cycle. Second law efficiency and total annual cost of the cascade refrigeration system are chosen as design objectives to be optimized individually and concurrently in order to obtain the optimal operating conditions of the system. Single optimization results show that R744/R1234yf system has the lowest operating cost while having the highest second law efficiency compared to other cycle configurations. A set of non-dominated solutions obtained through multi objective Artificial Cooperative Search algorithm is represented in the form of Pareto front and the best result is chosen from the well-reputed decision makers of TOPSIS and LINMAP for each cycle configuration. Multi objective optimization results reveal that design variables of the refrigeration system can create a trade off between problem objectives. A sensitivity analysis is performed to investigate the influences of varying values of design variables upon problem objectives while the system is operated under optimal conditions.

Nomenclature

A	Heat transfer area (m^2)
B	Baffle spacing (m)
Bo	Boiling number
$C_{capital}$	Capital cost ($)
C_{el}	Unit electricity cost ($)
C_p	Specific heat (kJ/kgK)
C_{rat}	Compression ratio
COP	Coefficient of performance
CRF	Capital Recovery Factor
D_s	Shell diameter (m)
d	Tube and fin diameter (m)
Fa	Fang number
G	Mass flux (kg/m^2s)
g	Gravitational acceleration (m/s^2)
H	Height (m) – Annual working hour of the system component (hour)
h	Heat transfer coefficient (W/m^2K) - Enthalpy (J/kg)
h_{fg}	Enthalpy of vaporization (J/kg)
i	Interest rate (%)
k	Thermal conductivity (W/mK)
L	Length (m)
$\dot{m}$	Mass flow rate (kg/s)
N_p	Number of tube pass
n	Number of tube rows in the pack - Operating period of the system
P_t	Tube pitch (m)
P_f	Fin pitch (fin/m)
Q	Heat flow (W)
Pr	Prandtl number
R	Fouling resistance (m^2K/W)
Re	Reynold number
s	Entropy (kj/kgK)
T	Temperature (°C - K)
ΔT_{LM}	Mean logarithmic temperature difference
ΔT_{CAS}	Temperature difference in the cascade condenser
T_0	Ambient temperature (K)
t	Tube thickness (m)
U	Overall heat transfer coefficient (W/m^2K)
W	Compressor power (kW)
X_{tt}	Martinelli parameter

✉ Mert Sinan Turgut
sinanturgut@me.com

[1] Mechanical Engineering Department, Ege University, 35040 Bornova, İzmir, Turkey

x Vapor quality
Z Capital cost ($)

Greek Symbols

δ Fin thickness (m)
ε Void fraction
η_{II} Second law efficiency
η_{is} Isentropic compressor efficiency
η_C Mechanical compressor efficiency
θ Maintenance factor
μ Dynamic viscosity (Pa.s)
ρ Density (kg/m^3)
σ Surface tension (N/m)

Subscripts

C – cond Condenser
E – evap Evaporator
HTC High temperature circuit
H Hot temperature medium
in Inner
LTC Low temperature circuit
L Low temperature medium
l Liquid
out Outer
tp Two phase
v-g Vapor

1 Introduction

Single stage vapor compression cycles are widely accepted refrigeration systems, those have been successfully utilized in many areas of industrial applications ranging from food industries to air conditioning systems. However, these type of refrigeration systems are not beneficial and economical for low temperature applications due to their inherent shortcomings such as low operating pressures of working fluids, and inefficiencies of the running compressors which are charged with refrigerants with large specific volumes [1]. In addition, a refrigeration medium with a huge temperature difference between hot and cold sides entails a reduction in evaporation pressures, which causes unexpected air leakages into the system. A promising alternative to overcome these operational drawbacks is using the merits of the cascade refrigeration cycle in which two or more vapor compression cycles are coupled to each other by means of a cascade condenser. Cascade condenser acts as a condenser for low temperature cycle and serves as an evaporator for high temperature cycle. Earlier design of cascade systems involves HCFC and HFC refrigerants such as R12, R134a, and R404a, etc. However, hazardous effects of these artificial refrigerants to the environment has restricted their utilization in refrigeration systems. Researchers propose a favorable solution to this problem through utilizing natural substances (CO_2, NH_3, Propane, etc.) instead of HFC - based refrigerants for chilling purposes [2]. Main reason behind this proposed substitute is high global warming potential rates of the synthetic refrigerants and destruction occured on the ozone layer resulted by their extravagant usage in different industrial applications.

Although CO_2 has been used in vapor compression systems for about 130 years [3], Lorentzen and Petterson [4] pioneered the extensive usage of CO_2 as a natural refrigerant, relying upon its major advantages such as non-explosive, non-toxic, eco-friendly behaviours accompannied by its favorable thermo-physical characteristics which allows its utilization in low temperature refrigeration applications. Ammonia is another natural refrigerant having plenty of application in industrial and commerical refrigeration appliances. In spite of not being faithfully recommended due to its inherent high toxicity and large compressor work requirements at operating temperatures under −35 °C, its abundance in nature and relatively low flammability convince researchers to use it as a refrigerant in low temperature two stage refrigeration systems [4, 5]. A cascade refrigeration system operated with CO_2/NH_3 working pair has drawn considerable interest from researchers as these two refrigerants have complementary thermal characteristics those enabling them to compansate the inherent deficiencies of both ammonia and carbon dioxide. Dopazo et al. [6] investigated the applicability of CO_2/NH_3 refrigerant pair on respectively low and high temperature circuits. They obtained an optimum CO_2 condensing temperature based on energy and exergy optimization. Dokandari et al. [7] themodynamically analyzed the utilization of an ejector in cascade refrigeration cycle working with CO_2 and NH_3 refrigerants. Theoretical analysis concerning the effects of ejector usage on overall system performance revealed that there is a significant improvement on first and second law efficiencies compared to the conventional vapor compression refrigeration systems.

As previously mentioned above, environmental problems such as global warming and ozone depletion mostly occured by the use of HFC and HCFC based synthetic rerfigerants have reached severity levels in the last decade. Most of the vapor compression system today in use work with the refrigerants having zero ozone depletion potential (ODP = 0). Nevertheless, nearly all of them have relatively high global warming potential rates. For instance, R134a, which is the most popular and applied refrigerant in air conditioning and refrigeration system, has a GWP of 1300 [8]. EU Commission Directive put a restrictive ban on the utilization of the refrigerants with a GWP higher than 150 in mobile air conditioners. As a possible replacement for R134a, designers and manufacturers propose using CO_2 and R1234yf (HFO-1234yf) instead of R134a because of their low GWP values of 1.0 and 4.0, correspondingly. SAE report [9] claims the idea that R1234yf is the best possible replacement for R134a. Nucleate boiling heat transfer characteristics of R134a and R1234yf for plain and low fin surfaces were compared in the work of Park and Jung [10]. They also concluded that any flow boiling correlation developed for R134a can be conveniently utilized for the thermal design of evaporators as well as boilers operated with

R1234yf. There are several literature studies indicating that refrigeration performance of R134a is better than that of R1234yf in chiller systems [11–15]. However, most of them also reported that among available alternative low GWP refrigerants, using R1234yf as a substitute for R134a would be more realistic and beneficial to environment as its contribution to global warming is much lower than the others. Comprehensive literature review on possible replacement of R1234yf instead of R134a reveals that although there has been many published studies on this hot spot research area, their comparative performance evaluation on cascade refrigeration systems in terms of both exergetic and economic point of view has not been adequately investigated yet. In addition, it is also seen that there has been limited research studies dealing with both thermoeconomic and exergetic optimization of cascade refrigeration cycles [16, 17]. Most of the studies in the literature evaluate the cycle efficiency in terms of themodynamic aspects. This type of cycle efficiency evaluation leads to attainment of maximum coefficient of performance or minimum exergy destruction. However, this may result into the occurence of enormous increases in total cost of the system. Therefore, thermoeconomic considerations should be taken into account in order to make a plausible and cost-effective cycle design. A thermodynamic cycle which is thermoeconomically optimized has design variables obtained by the trade-off between energy and capital costs. Aminyavari et al. [16] analysed the applicability of CO_2/NH_3 cascade refrigeration cycle with regard to thermoeconomic, exergetic, and environmental aspects. Multi objective optimization made through genetic algorithm was employed to obtain optimum design paramters of the considered cascade refrigeration system. Design objectives of exergetic efficiency and total cost of the system were simultaneously optimized by multi objective genetic algorithm and best answer from the non dominated solution was obtained by TOPSIS decision making method. Rezayan and Behbahaninia [17] made thermoeconomic and exergetic optimization of two stage refrigeration cycle operated with CO_2/NH_3 refrigerant pair. Design variables to be optimized were selected as condensing temperatures of carbon dioxide and ammonia, evaporation temperature of carbon dioxide, and temperature difference between working refrigerants in hot and cold circuits.

This study aims to make comparative investigation on optimum operating conditions of R744-R717, R744-R134a, and R744-R1234yf cascade refrigeration cycles based on thermoeconomic and exergetic point of view. After modelling of the two stage refrigeration system for each refrigerant pair, dual design objectives of minimum total cost of the system and maximum second law efficiency will be optimized in a single and multi-objective manner. Artifical Cooperative Search [18] metaheuristic optimization algorithm is simultaneously applied to above mentioned design objectives in order to find optimum system decision variables of condenser and evaporation temperatures, R744 condensation temperature, temperature difference between two working fluids in the cascade temperature, amount of superheating and subcooling in the hot and cold circuits. To the authors' best knowledge, this is the first multi objective optimization of R744-R134a and R744-R1234yf cascade cycles. In addition, this study will be the first detail examination on possible replacement of R1234yf instead of R134a in cascade refrigeation cycles. Optimal results of these two refrigeration system will be compared with those obtained from R744-R717 cascade system, which is the most applied refrigerant pair on cascade refrigerant cycles. After applying optimization method to each problem objective concurrently, a set of optimal solution called "Pareto front" will be achieved for each cycle configuration. Two well-reputed decision making methods, namely, TOPSIS and LINMAP are utilized to choose final design point amongst the non-dominated solutions represented in the Pareto frontier. Influences of the variation of design variables on problem objectives will be analysed through parametric analysis. A sensitivity analysis will be then performed to observe the variational effects of the imposed cooling load on the Pareto frontier.

2 Mathematical modelling of the cascade refrigeration system

Figure 1 demonstrates the schematic representation of the cascade refrigeration cycle considered for this study. System

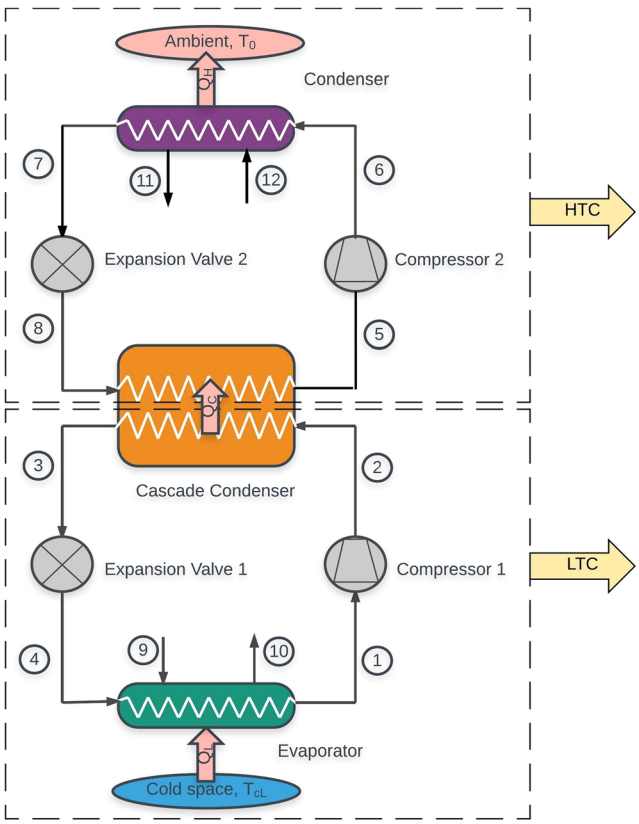

Fig. 1 Schematic representation of cascade refrigeration system

comprises two seperated single vapor compression refrigeration cycles including low temperature (LTC) and high temperature circuits (HTC). R134a, R1234yf, and R717 are seperately utilized as refrigerant for hot side while R744 is used in cold side for each cycle configuration. Each circuit comprises an extension valve, an evaporator, a compressor and a condenser These two seperate circuits are coupled to each other by means of a cascade condenser which perform as a condenser for the low temperature circuit and evaporator for high temperature circuit.

Imposed cooling load $\dot{Q}_L$ is absorbed from cooling space by the evaporator in the low temperature circuit (LTC) at the evaporation temperature of T_E. HTC condenser at temperature T_C rejects the process heat $\dot{Q}_H$ into the ambient having the temperature of T_0. Condenser in the LTC at temperature of T_{CC} rejects the heat to the evaporator in HTC at temperature T_{EC} through cascade condenser. The transferred heat in cascade condenser is the sum of the work input $\dot{W}_{LTC}$ to the compressor in LTC and the imposed cooling load $\dot{Q}_L$ in LTC. In the same manner, the heat $\dot{Q}_H$ rejected to the ambient is the summation of input compressor work $\dot{W}_{HTC}$ required for HTC and the absorbed heat $\dot{Q}_C$ by the evaporator of HTC. Temperature difference between phase changing refrigerants in the cascade condenser is represented by $\Delta T_{CAS}(=T_{EC}-T_{CC})$.

Each cycle component given in Fig. 1 can be considered as a single control volume for the sake of simplicity in evaluation of thermodynamic relations. Thermodynamic analysis on the two stage refrigration cascade system is grounded based on the below given assumptions:

- Kinetic and potential changes in each single cycle component are negligible
- All pressure and heat losses in the piping network or cycle component are disregarded
- Cycle components are assumed to be operated under steady-state flow conditions.
- Each compressor in the cycle has a combined mechanical and motor efficiency of 0.93 [3]
- Throttling valves in the cycle are assumed to be isenthalpic

Numerical analysis are performed by using fundamental thermodynamical balance equations with taking into consideration of above mentioned assumptions, in order to obtain the amount of heat transfer through condenser and cascade-condenser, the compressor work, and the mass flow rate in each cyle component.

Mass balance equation

$$\sum_{in}\dot{m}=\sum_{out}\dot{m} \tag{1}$$

Energy balance equation

$$\dot{Q}=\dot{W}+\sum_{out}\left(\dot{m}\cdot h\right)-\sum_{in}\left(\dot{m}\cdot h\right) \tag{2}$$

Table 1 reports the detailed formulations of each above given fundamental equation for each cycle component. Thermophysical properties of the working fluids used in this study are determined by the freeware software package CoolProp [19]. Isentropic efficiency of the CO_2 compressor is obtained as a function of compression ratio in LTC with the following correlation [20].

$$\eta_{is}=0.00476C_{rat}^2-0.09238C_{rat}+0.89810 \tag{3}$$

Isentropic efficiencies of the high temperature circuit refrigerants of R717, R134a, R1234yf are expressed with below given correlations:

R717 Compressor [21].

$$\eta_{is}=-0.00097C_{rat}^2-0.01026C_{rat}+0.83955 \tag{4}$$

R134a and R1234yf Compressors [16].

$$\eta_{is}=1.0-0.04C_{rat} \tag{5}$$

Coefficient of performance (COP) of the cascade refrigeration system is expressed by the following equation

$$COP=\frac{\dot{Q}_L}{\dot{W}_{LTC}+\dot{W}_{HTC}} \tag{6}$$

Exergetic efficiency of the whole refrigreation system can be represented as a function of actual COP and Carnot COP with the following equation form [3]:

$$\eta_{II}=\frac{COP}{COP_{carnot}} \tag{7}$$

Where Carnot COP is calculated by

$$COP_{carnot}=\frac{T_E}{T_C-T_E} \tag{8}$$

2.1 Heat exchanger modelling

A plate fin heat exchanger is considered for the evaporator and the condenser, while a shell and tube heat exchanger is used for the cascade condenser. Generally, heat ransfer mechanism of condenser and evaporator consists of air convection, heat conduction through tubes, and two phase convection of working fluid. Air fin evaporator and condenser is used for heat exchange between hot and cold mediums as these type of heat exchangers have lower maintenance cost, lower pressure drops, higher thermal efficiency, lower fan power consumption, and higher corrosion resistance [22]. Mathematical modelling of induced draft air fin coolers is not given in this study due to the space restriction. However, interested readers could find the detailed explanation of the heat transfer modelling of an air fin cooler in [23].

Table 1 Thermodynamic equations used to model cascade refrigeration cycle

Component	Mass balance equation	Energy balance equation	
Low temperature circuit			
Evaporator	$\dot{m}_4 = \dot{m}_1 = \dot{m}_{LTC}$	$\dot{Q}_L = \dot{m}_{LTC}(h_1 - h_4)$	
Compressor	$\dot{m}_1 = \dot{m}_2 = \dot{m}_{LTC}$	$\dot{W}_{LTC} = \frac{\dot{m}_{LTC}(h_2 - h_1)}{\eta_C}$	
Expansion valve	$\dot{m}_3 = \dot{m}_4 = \dot{m}_{LTC}$	$h_3 = h_4$	
High temperature circuit			
Condenser	$\dot{m}_6 = \dot{m}_7 = \dot{m}_{HTC}$	$\dot{Q}_H = \dot{m}_{HTC}(h_6 - h_7)$	
Compressor	$\dot{m}_5 = \dot{m}_6 = \dot{m}_{HTC}$	$\dot{W}_{HTC} = \frac{\dot{m}_{HTC}(h_6 - h_5)}{\eta_C}$	
Expansion valve	$\dot{m}_7 = \dot{m}_8 = \dot{m}_{HTC}$	$h_7 = h_8$	
Cascade condenser	$\dot{m}_5 = \dot{m}_8 = \dot{m}_{HTC}$ $\dot{m}_2 = \dot{m}_3 = \dot{m}_{LTC}$	$\dot{Q}_{CAS} = \dot{m}_{HTC}(h_6 - h_7)$	$= \dot{m}_{LTC}(h_2 - h_3)$

Effective heat exchanger design also needs elaborate definition of system parameters such as number of tubes in the bundle, tube diameter, shell diameter, etc. Table 2 and Table 3 respectively report the design parameters of condenser, evaporator, and cascade condenser used in this study. The flow boiling correlations used in this study are Gungor and Winterton [24], Fang [25] and Fang [26] and in-tube condensation correlations are Cavallini et al. [27], Fronk and Garimella [28] and Kern [29]. Mentioned correlations are considered based on their predictive performances, which were evaluated in past literature studies [25, 26, 30, 31]. Detailed discussion will be made in upcoming sections as to why these correlations are considered for modelling of the heat exhangers on cold and hot sides. On the grounds of the above given definitions and explanations, total heat exchange surface of the each heat exchanger in the refrigeration cycle is computed by the following equation

$$A_o = \frac{\dot{Q}}{U_o \cdot \Delta T_{LM}} \tag{9}$$

Where ΔT_{LM} is the mean logarithmic temperature difference and U_o is the overall heat transfer coefficient expressed based on the outside heat exchange area

$$U_o = \frac{1}{\frac{d_{out}}{h_{in} \cdot d_{in}} + R_{f,in}\frac{d_{out}}{d_{in}} + d_{out}\frac{\ln(d_{out}/d_{in})}{k_w} + R_{f,out} + \frac{1}{h_{out}}} \tag{10}$$

2.2 Economic analysis

One of the major aims of this study is to evaluate economic analysis of the cascade refrigeratin cycle based on the capital and operational costs of the system components operating under specific conditions. Cost of the expansion valves is not included into total expenditure cost of the refrigeration system due to their negligible cost rates compared to other system components. Total cost of the cascade refrigeration system (C_{total}), consisting of the capital and maintenance costs ($C_{capital}$) and the operating cost (C_{oper}),

$$C_{total} = C_{capital} + C_{oper} \tag{11}$$

Table 2 Design parameters of the air fin condenser and evaporator

	Condenser	Evaporator
Height – H (m)	0.3	0.3
Length – L (m)	0.5	0.5
Tube pitch – P_t (m)	0.053975	0.053975
Fin pitch – P_f (fin/m)	354	346
Fin thickness – δ (m)	0.0004826	0.0004826
Fin inside diameter – d_b (m)	0.0027432	0.0027432
Fin outside diameter – d_a (m)	0.0050800	0.0050800
Liner inner diameter – d_i (m)	0.0220980	0.0220980
Liner outer diameter – d_o (m)	0.0254000	0.0254000
Gap outside diameter – d_g (m)	0.0026467	0.0026467
Thermal conductivity of tubes – k_t (W/m.K)	200.0	200.0
Number of tube rows in the pack – n_r	6.0	6.0
Fouling resistance – R_f (m^2.K/W)	0.00044	0.00044

Table 3 Design specifications of the shell and tube cascade condenser

Tube outside diameter – d_{out} (m)	0.016
Tube thickness – t (m)	0.002
Number of tube passes – N_p	1.0
Shell diameter – D_s (m)	0.3
Baffle spacing – B (m)	0.2
Thermal conductivity of the tubes (W/mK)	200.0

Below given mathematical relations can be used for estimating the capital cost of the each cycle component (except for expansion valves) [16, 31].

$$Z_{HTC,comp} = 9624.2W_{HTC,comp}^{0.46} \tag{12}$$

$$Z_{LTC,comp} = 10167.5W_{LTC,comp}^{0.46} \tag{13}$$

$$Z_{cond} = 1397A_{cond}^{0.89} + 629.05\dot{W}_{fan,cond}^{0.76} \tag{14}$$

$$Z_{cond} = 1397A_{evap}^{0.89} + 629.05\dot{W}_{fan,evap}^{0.76} \tag{15}$$

$$Z_{cas,cond} = 2382.9A_{cas,cond}^{0.68} \tag{16}$$

Capital Recovery Factor (CRF) is a simple equation defined to calculate the actual present value of the annuity. CRF converts the actual cost value into a series of equal annular payments at specific interest rate for a predefined time period. Its formulation can be given as

$$CRF = \frac{i(1+i)^n}{(1+i)^n - 1} \tag{17}$$

In which the parameters i and n correspondingly represent the interest rate and total operating time of the system in years. Having calculated the CRF, total capital cost is converted into the annulized form by the following equation

$$C_{capital} = \sum_i Z_i \cdot CRF \cdot \theta \tag{18}$$

Where θ is the maintenance factor. Finally, total capital and maintanence cost of the cascade refrigeration system is computed by applying Eq. (18) to each system component

$$\sum_i Z_i = Z_{cas,cond} + Z_{evap} + Z_{cond} + Z_{LTC,comp} + Z_{HTC,comp} \tag{19}$$

Operational costs are concerned with the electricity consumption made by compressors and fans of the refrigeration system, and mathematically expressed by the following equation

$$C_{oper} = \left(\dot{W}_{LTC,comp} + \dot{W}_{HTC,comp} + \dot{W}_{LTC,fan} + \dot{W}_{HTC,fan}\right) \cdot C_{el} \cdot H \tag{20}$$

Where C_{el} is the unit cost of the electricity and H is the total working hours per year.

3 Multi objective optimization

Multi objective optimization deals with the real world optimization problems with having contradictory design objectives involving equality and inequality constraints. Many conventional optimization algorithms are available to be utilized on multi objective optimization problems [32–35]. However, they inherit some drawbacks such that slow and premature convergence may sometimes happen due to the algorithmic complexity. Optimization performance of Newton-based methods is also questionable due to the strong dependence of initial conditions. Additionally, if gradient based methods are put into practice, they generally stuck into local optimum points due to the undifferentiable points in the search domain. Metaheuristic algorithms can be a useful alternative to circumvent the inherent disadvantages of the conventional optimization methods since it is shown in many studies that they have the capability of solving high dimensional and extremely nonlinear optimization problems. Metaheuristics are problem-independent solution strategies that provide a specific framework to construct heuristics. Some examples of famous metaheuristc algorithms are Genetic algorithm [36], Ant colony optimization [37], Harmony search [38, 39], etc. Metaheuristics are efficient problem solvers those having the capability of maintaining a successfull balance between computation time and solution quality. Literature comprises many applications of multi objective metaheuristic algorithms on the design of thermodynamic systems involving more than one problem objectives to be concurrently optimized [40–45]. This study considers Artificial Cooperative Search metaheuristic algorithm to accomplish simultaneous optimization of two conflicting problem objectives including minimum total cost and maximum second law efficiency of the cascade refrigeration system. Artificial Cooperative search algorithm gave very satisfactory results in past studies [45, 46] and mostly outperformed its competitors in terms of solution quality, which is why this algorithm is considered for this study.

Multi objective optimization aims to obtain set of optimal solutions those are non-dominated to each other. Each solution on the frontier is equally important and it is not possible to improve any objective without sacrifising to others. That is to say, there is no mathematical best solution along the curve. These points on the curve are called Pareto solutions. Pareto solutions represent a trade-off between problem objectives and give options to designers to choose a possible answer to his or her design requirements. Assuming that n number of functions to be simultaneously optimized, multi objective optimization problem can be expressed as

$$\text{Maximum/Minimum}\left[f_1\left(\vec{x}\right), f_2\left(\vec{x}\right), \ldots, f_n\left(\vec{x}\right)\right]^T \tag{21}$$

With subject to

$$g_j\left(\overrightarrow{x}\right) \leq 0 \quad \forall j = 1, 2, .., M \tag{22}$$

$$h_k\left(\overrightarrow{x}\right) = 0 \quad \forall k = 1, 2, \ldots, K \tag{23}$$

$$x_d^L \leq x_d \leq x_d^U \quad d = 1, 2, \ldots, D \tag{24}$$

Where $f_1\left(\overrightarrow{x}\right), f_2\left(\overrightarrow{x}\right), \ldots, f_n\left(\overrightarrow{x}\right)$ are n problem objectives to be concurrently optimized; $\overrightarrow{x} = [x_1, x_2, \ldots, x_D]$ is D-dimensional solution vector restricted between upper (x^U) and lower (x^L) bounds of the search space. There are M inequality constraints $g_j\left(\overrightarrow{x}\right)$ and K equality constraints $h_k\left(\overrightarrow{x}\right)$ in the multi objetive optimization problem.

As mentioned before, Pareto curve consists of nondominated trial solutions which are possible candidates for final answer to optimization problem. This study simultaneously uses two well-reputed decision making methods of LINMAP and TOPSIS to choose final optimum solution among the possible alternatives. LINMAP and TOPSIS decision makers use distance metrics to correctly measure the Euclidian distance between ideal/nadir solution and each trial solution in the frontier. All objectives must be rescaled and unified before application of decision making methods. Therefore, problem objectives should be non-dimensionalized with using available methods in the literature. This study uses Euclidian approach, which is defined as the following equation

$$F_{ij}^t = \frac{F_{ij}}{\sqrt{\sum_{i=1}^{k} \left(F_{ij}\right)^2}} \tag{25}$$

F_{ij} stands for the problem objectives at various optimum points on the pareto curve; i represents the index of the solution points on the curve; and j symbolizes the index of each objective on the frontier. TOPSIS and LINMAP decision making methods will be briefly explained in the upcoming sections.

3.1 LINMAP decision maker

LINMAP method evaluates the Euclidian distance between the ideal point and each solution on the pareto curve with the following equation.

$$d_{i+} = \sqrt{\sum_{j=1}^{k} \left(F_{ij} - F_j^{ideal}\right)^2} \tag{26}$$

Where k denotes the number of problem objectives; i ($i = 1, 2, .., m$) represents each optimal solution on the Pareto front; F_j^{ideal} is the optimum solution of the j^{th} problem objetive obtained by single objective optimization. Optimal solution whose spatial distance to ideal point is the most closest is selected as the final optimum solution. That is

$$i_{final} = i \in \min(d_{i+}) \tag{27}$$

Where i is the index of the final optimum solution.

3.2 TOPSIS decision maker

Apart from the ideal point, nadir point is also considered in TOPSIS decision making theory. Nadir point is the solution of each design objective with having the worst functional value. The computation of the Euclidian distance between each nondominated solution on Pareto curve and nadir point is expressed by the following equation

$$d_{i-} = \sqrt{\sum_{j=1}^{k} \left(F_{ij} - F_j^{nadir}\right)^2} \tag{28}$$

Based on equation Eqs. (26) and (28), a parameter Cl_i is defined as the following expression

$$Cl_i = \frac{d_{i-}}{d_{i-} + d_{i+}} \tag{29}$$

After applying Eq. (29) to each solution on the frontier, a desired final answer is selected by choosing the solution with having maximum value of Cl_i. This definition can be mathematically expressed as

$$i_{final} = i \in \max(Cl_i) \tag{30}$$

Where i_{final} denotes the index of the final optimal solution.

4 Verification of the developed model

The cascade refrigeration model is developed in Java with using Coolprop. Coolprop environment is an open source library which uses variety of the developed theoretical and empirical models available in the literature for estimation of the thermophysical properties of pure and mixture refrigerants. Considered optimization parameters such as exergy efficiency and total cost of the cascade refrigeration system obtained from this study have been benchmarked against the results reported in [6]. Figure 2 visualizes the comparison between the given results in the corresponding reference and the model results found in this study. It is seen that the achieved model outcomes are in line with those found in the reference study.

Another verificiation should be made on the prediction accuracy of the two phase flow heat transfer correlations used for estimating the heat transfer rates in the evaporator and condenser. Most of these two phase flow heat transfer correlations are developed for specific refrigerants for their own measurements.

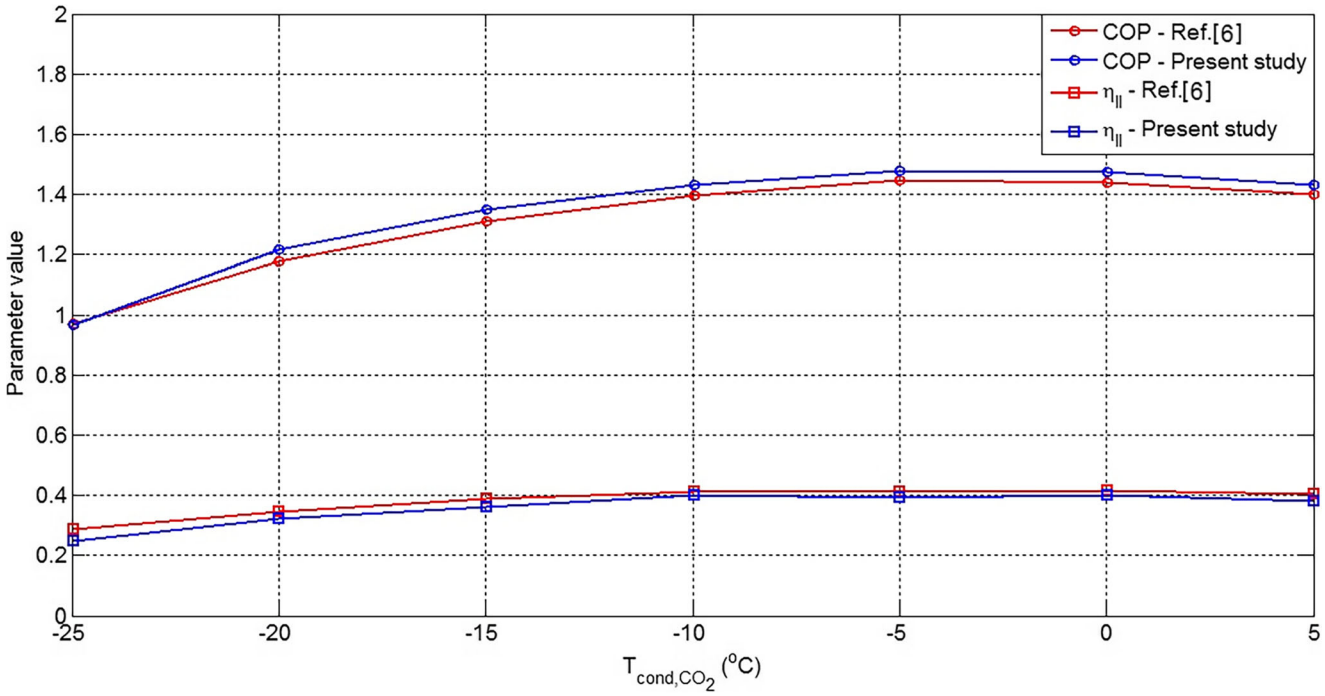

Fig. 2 Performance assessment of the developed thermodynamic model with the reference literature study [6]

Therefore, their predictive performance is in question when they have been practiced out of the limits of their application domain. This study aims to benefit the favourable merits of the refrigerant specific two phase flow heat transfer correlations, relying upon their well-established heat transfer coefficient estimation capabilities. As mentioned in the past literature studies [47, 48], thermophysical properties of R134a are very close and similar to those of R1234yf. Therefore, correlation of Fang [26] which was developed based on R134a experimental data, has been applied to both R134a and R1234yf to determine their corresponding flow boiling heat transfer coefficients. In the work of Wang et al. [30], it was revealed that Gungor Winterton correlation [24] gives the best performance in predicting the convective boiling heat transfer of R717 for macro tubes. Due to the peculiar thermophysical properties of R744, existing flow boiling correlations generally fails the estimate the actual heat transfer values of carbon dioxide when two phase flow prevails in the flow channels. Fang [25] proposed a R744 based flow boiling correlation in order to make a progress in improving prediction accuracy. Proposed correlation outperforms the avaliable counterparts in terms of estimation performance. According to the review paper [12] in which prediction accuracy of the in-tube condensation correlations were scrutinized, Cavallini et al. [27] correlation gives the best performance for smooth tubes. There are also several experimental studies [49–51] verifying the superiority of the correlation of Cavallini et al. [27] over its counterparts with respect to the accuracy of the estimated heat transfer coefficient values. Although using ammonia as a working fluid in condensers has many potential benefits, very limited research study has been performed concerning the intube flow condensation of this refrigerant. As a result of this, existing correlations have failed to estimate the actual heat transfer rates. Among these correlations, ammonia based intube flow condensation correlation developed by Fronk and Garimella [52] provide a reliable prediction accuracy and stand out amongst the other methods. All above mentioned correlations have been utilized in this study in calculating two phase heat transfer values due to their superior performance and extreme prediction capabilities. Figure 3 shows the deviations between the experimental data consolidated from the literature and the calculated heat transfer coefficient values obtained from refrigerant specific correlations. It is seen that most of the experimental data fall within ±25% error zone for both condensation and evaporation cases. Such conclusion can be drawn from the figure that it is reliable to use the above mentioned correlations in heat exchanger design calculations.

5 Results and discussion

Multi objective Artificial Cooperative Search algorithm is applied to optimal design of three different cascade refrigeration cycle operated with R744/R717, R744/R134a, and R744/R1234yf refrigerant pairs. Second law efficiency and total annual cost of the cascade refrigeration system are chosen as design objectives to be optimized in a single and multi objective manner. Air fin evaporator and condenser are respectively used at cold and hot sides as an heat exchange medium while shell and tube heat exchanger is utilized as cascade condenser. Table 4 gives the decision variables to be optimized to obtain

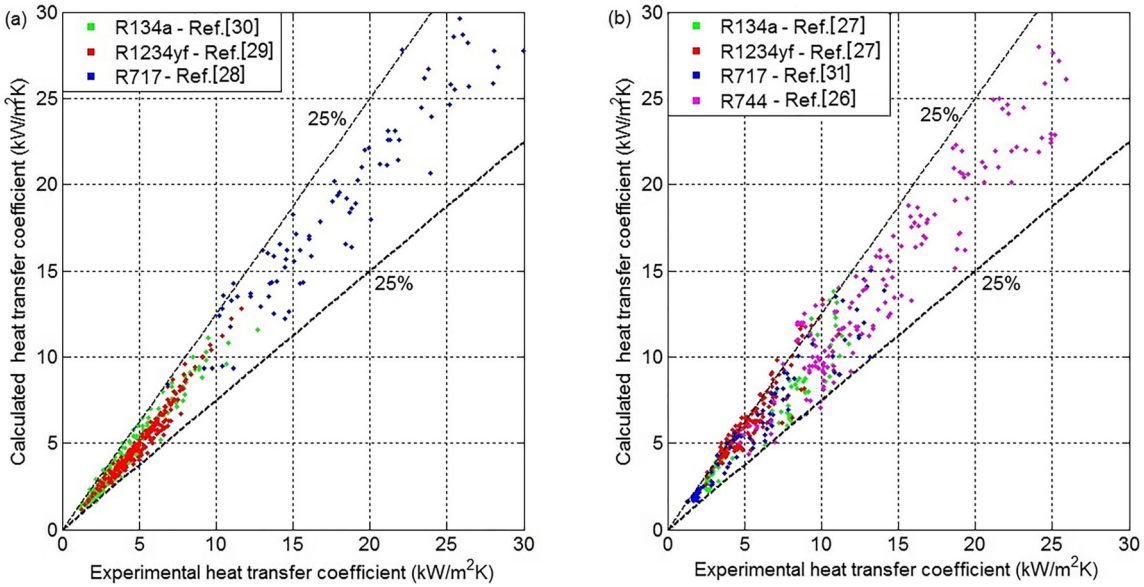

Fig. 3 Comparison of the heat ransfer coefficient rates obtained from two phase correlations and experimental data consolidated from literature: **a** In-tube condensation **b** In-tube flow boiling

the optimal performance of the refrigeration system. Evaporator temperature, condenser temperature, condensing temperature at the cascade condenser, temperature difference in the cascade condenser, amount of subcooling and overheating in hot and low temperature circuits are considered as design variables relying on their strong influences of system performance [17].

Table 5 reports the operational parameters of the refrigeration system. Table 6 reports the optimal results found for the cascade refrigeration system working with R744/R717 refrigerant pair. Single optimization results reveal that optimal total annual cost value is found to be 41,920.843 $ while second law efficiency is 0.40845. Optimal second law efficiency is 0.46853 while total annual cost rates reaches up to 52,343.313 $. One can observe the correlation between overall COP and second law efficiency of the system since COP values are increased with increasing second law efficiency rates. Amount of subcooling and overheating in the bottom cycle nearly hit its upper limits in both optimization cases. However, amount of overheat in top cycle is at its lower limit while subcooling temperature reaching its upper limits. Drastic increases are seen in heat exchange areas of the cascade condenser (increased by 628%) and evaporator (increased by 134.1%) when optimization objective is switched from minimum total annual cost to maximum second law efficiency. Contrary to this tendency, required compressor power for hot and low temperature circuits and total heat exchange area of the condenser decrease when second law efficiency is optimized instead of the total annual cost of the refrigeration system. It can be observed from Table 6 that when minimum total annual cost is achieved, second law efficiency rates are far away from their optimal values or vice versa. This behavior clearly shows the conflicting nature between two problem objectives, therefore multi objective optimization is put into practice in this study to obtain a comprimise solution through multi objective Artifical Cooperative Search metaheuristic algorithm.

Figure 4 shows the pareto curve along with the pareto optimal solution obtained by TOPSIS and LINMAP decision making methods for R744/R717 cascade refrigeration system. Both methods find the same optimal results, which is also reported in Table 6. Pareto optimal value of the total annual cost and second law efficiency is respectively 41,924.976 $ and 0.40913 as reported in Table 6, which is very close to the minimization

Table 4 Upper and lower bounds of the defined search domain

	Lower	Upper
Evaporator temperature (°C)	−40.0	−30.0
Amount of overheat at the low temperature cycle (°C)	0.0	5.0
Amount of subcooling at the low temperature cycle (°C)	0.0	5.0
Temperature difference in the cascade condenser (°C)	2.0	8.0
Condensing temperature of R744 in the cascade condenser (°C)	−5.0	5.0
Condenser temperature (°C)	30.0	40.0
Amount of overheat at the high temperature cycle (°C)	0.0	5.0
Amount of subcooling at the high temperature cycle (°C)	0.0	5.0

Table 5 Operational parameters of the cascade refrigeration system

Cooling rate (kW)	40.0
Ambient temperature (°C)	15.0
Air inlet temperature at the cold side (°C)	−35.0
Air outlet temperature at the cold side (°C)	−40.0
Air inlet temperature at the hot side (°C)	15.0
Air inlet temperature at the hot side (°C)	22.0
Equipment lifetime (year)	15.0
Maintenance factor	1.06
Annual interest rate (%)	14.0
Hours in operation per year	7000.0
Electricity cost ($/kWh)	0.07

results of total annular cost objective function. Figure 5 shows the variations of the considered design variables across the Pareto frontier demonstrated in Fig. 4. Figure 5 clearly reveals that evaporator temperature and temperature difference in the cascade cascade condenser are the only parameters varying between its upper and lower limits along the Pareto curve, which are the trade-off points causing conflict between problem objectives. Some variations are also observed for the values of condenser temperatures. Other design variables are accumulated at the vicinity of their prescribed maximum or minimum limits.

Single and multi objective optimization results of the cascade refrigeration cycle working with R744/R134a refrigerant pair are summarized in Table 7. Most of the decision variables nearly reach their upper and lower allowable limits for both single optimization cases. It is shown that overall COP of the

Table 6 Optimal operating conditions of the cascade refrigeration system working with R744/R717 refrigerant pair

	Minimum total cost	Maximum second law efficiency	Multiobjective optimization
Evaporator temperature (°C)	−37.935	−30.005	−37.872
Overheat temperature at the bottom cycle (°C)	4.999	4.962	4.998
Amount of subcooling at the bottom cycle (°C)	4.977	4.975	4.987
Temperature difference in the cascade condenser (°C)	7.389	2.012	7.312
Condensing temperature of R744 in the cascade condenser (°C)	−4.999	−4.986	−4.996
Condenser temperature (°C)	30.003	34.549	30.000
Amount of overheat at the top cycle (°C)	0.014	0.006	0.005
Amount of subcooling at the top cycle (°C)	4.988	4.962	4.998
System outputs			
Mass flow rate of R717 (kg/s)	0.047	0.044	0.047
Mass flow rate of R744 (kg/s)	0.151	0.150	0.150
Total heat exchange area of the evaporator (m^2)	56.073	131.265	56.413
Total heat exchange area of the cascade condenser (m^2)	13.682	19.296	13.981
Total heat exchange area of the condenser (m^2)	14.317	6.224	14.224
Required compressor power for the bottom cycle (kW)	11.685	7.957	11.648
Required compressor power for the top cycle (kW)	23.296	20.340	23.215
Overall COP (−)	1.414	1.764	1.418
Component cost			
Cost of the bottom cycle compressor ($)	31,501.747	26,397.836	31,455.791
Cost of the top cycle compressor ($)	40,956.244	38,477.599	40,890.249
Cost of the evaporator ($)	51,753.074	108,689.431	52,034.169
Cost of the condenser ($)	16,000.937	8113.125	15,913.511
Cost of the cascade condenser ($)	14,115.804	54,327.682	14,324.435
Total cost of the system components ($)	154,327.808	236,005.675	154,618.157
Problem objectives			
Total annual cost ($)	41,920.843	52,343.313	41,924.976
Second law efficiency (−)	0.40845	0.46853	0.40913

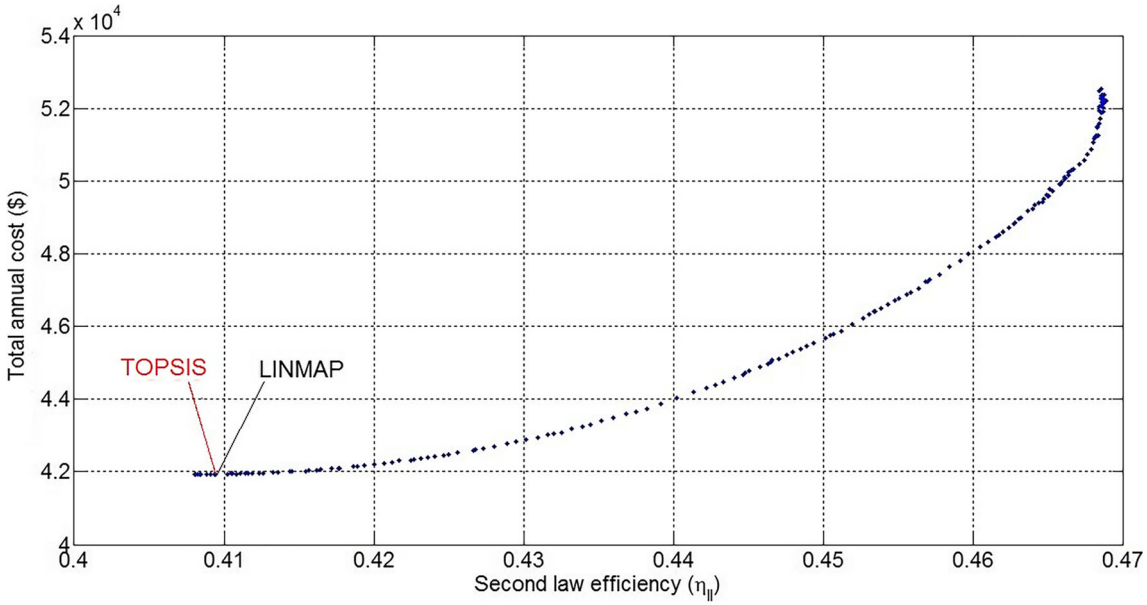

Fig. 4 Non-dominated pareto optimal solutions resulted from the multi objective optimization of the cascade refrigeration system operated with R744/R717 refrigerant pair

R744/R717 refrigeration system is higher than that of R744/R134a system when total annual cost minimization is under consideration, while the value of this parameter is higher compared to the R744/R717 refrigeration system when second law efficiency is individually optimized. Exergetic performance of R744/R717 refrigerant pair is slightly better than that of R744/R134a refrigeration system when second law efficiency is maximized. Contrary to this, total annual cost of R744/R134a cascade system is lower than that of R744/R717 cascade system when cost miminization is in practice. Readers can see the huge difference in the total heat exchange areas of the evaporator and condenser. This is not only because of the considerable difference between air side heat transfer coefficient values for cold and hot sides, but also the amount of the corresponding calculated two phase heat transfer coefficient rates for both evaporator and condenser. This explanation is valid for each mentioned refrigeration cycle in this study. Figure 6 visualizes the Pareto frontier constructed

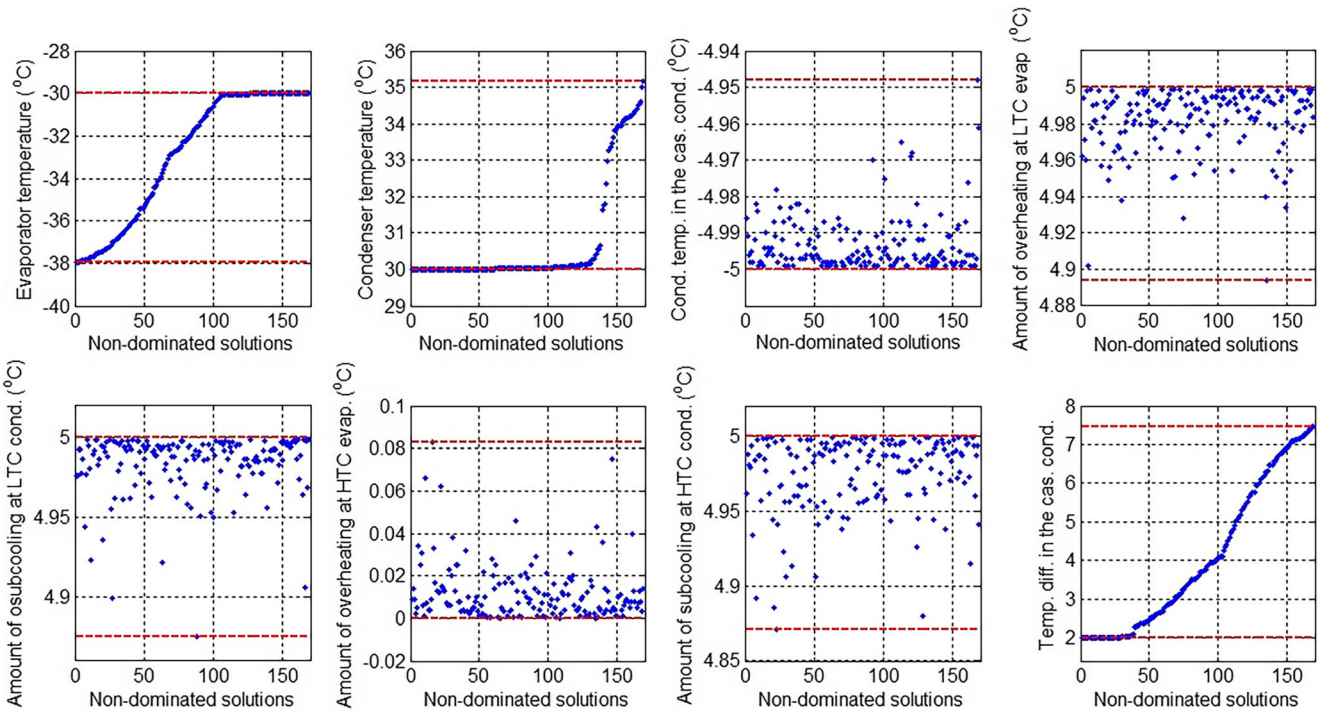

Fig. 5 Variation of system parameters along the Pareto curve constructed for optimum design of R744/R717 cascade cycle

Table 7 Optimal results for single and multi objective optimization of cascade refrigeration cycle working with R744/R134a refrigerant pair

	Minimum total annual cost	Maximum second law efficiency	Multiobjective optimization
Evaporator temperature (°C)	−39.977	−30.002	−39.811
Overheat temperature at the bottom cycle (°C)	0.073	0.161	0.021
Amount of subcooling at the bottom cycle (°C)	4.995	4.997	4.945
Temperature difference in the cascade condenser (°C)	2.043	2.006	2.007
Condensing temperature of R744 in the cascade condenser (°C)	−4.994	−4.967	−4.973
Condenser temperature (°C)	30.004	30.000	30.009
Amount of overheat at the top cycle (°C)	4.998	4.997	4.999
Amount of subcooling at the bottom cycle (°C)	4.993	4.999	4.990
System outputs			
Mass flow rate of R134a (kg/s)	0.331	0.296	0.330
Mass flow rate of R744 (kg/s)	0.154	0.153	0.153
Total heat exchange area of the evaporator (m^2)	61.150	182.281	62.116
Total heat exchange area of the cascade condenser (m^2)	13.142	11.710	13.301
Total heat exchange area of the condenser (m^2)	6.603	5.180	6.564
Required compressor power for the bottom cycle (kW)	15.045	9.002	14.943
Required compressor power for the top cycle (kW)	18.323	16.359	18.239
Overall COP (−)	1.367	1.851	1.375
Component cost			
Cost of the bottom cycle compressor ($)	35,385.554	27,939.292	35,274.208
Cost of the top cycle compressor ($)	36,672.961	34,809.647	36,596.005
Cost of the evaporator ($)	55,787.226	145,084.532	56,550.796
Cost of the condenser ($)	8553.598	7017.112	8512.198
Cost of the cascade condenser ($)	13,734.448	12,697.963	13,847.282
Total cost of the system components ($)	150,133.789	227,548.549	150,780.492
Problem objectives			
Total annual cost ($)	40,550.165	49,700.101	40,575.132
Second law efficiency (−)	0.41051	0.45680	0.41150

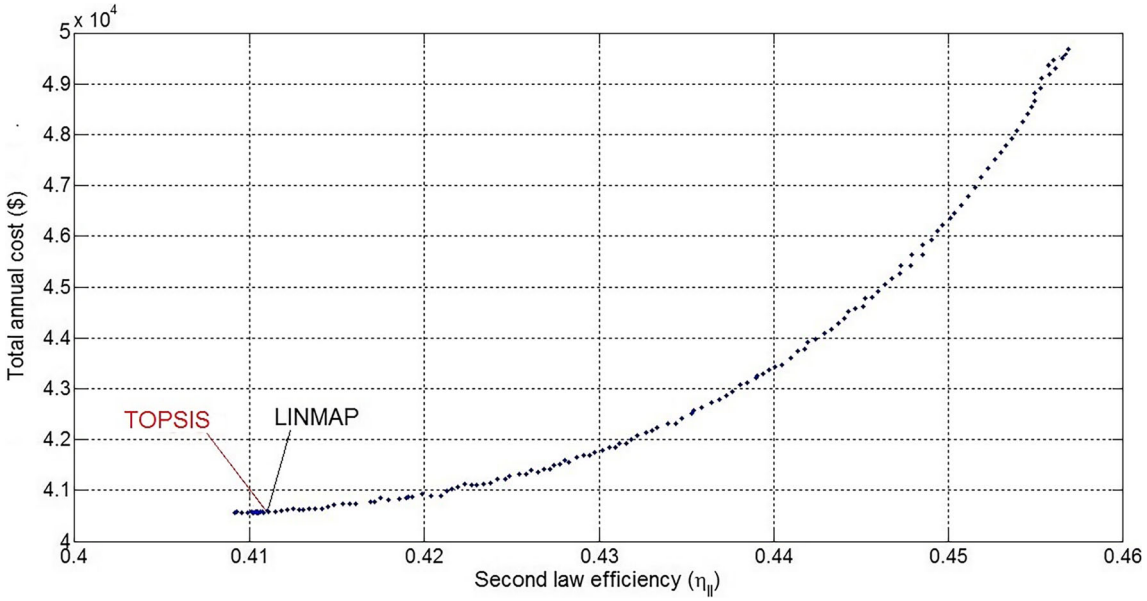

Fig. 6 Pareto curve constructed for R744/R134a cascade refrigeration cycle

for the optimum design of R744/R134a cascade refrigeration cycle, along with the optimal non-dominated solution attained by TOPSIS and LINMAP decision makers which is also reported in Table 7. Optimum values of total annual cost and second law efficiency are respectively 40,575.132 $ and 0.4115, according to the results obtained from TOPSIS and LINMAP theorems. It is seen that optimal solution is inclined towards lower total annual cost and second law efficiency values. Figure 6 also implies that as exergetic efficiency increases from 0.4105 to 0.4568, there occurs a marked increase in total annual cost of the refrigeration system, which is 22.66% of its initial value. Figure 7 demonstrates the variational distribution of the design parameters across the Pareto frontier built for the optimum design of R744/R134a cascade refrigeration cycle. Figure 7 shows that evaporation tempearture is the only decisive design parameter varying between its allowable limits, while others are nearly remaining constant throughout the Pareto curve. Thus, it can be concluded that evaporation temperature is the sole design parameter causing a trade-off between problem objectives.

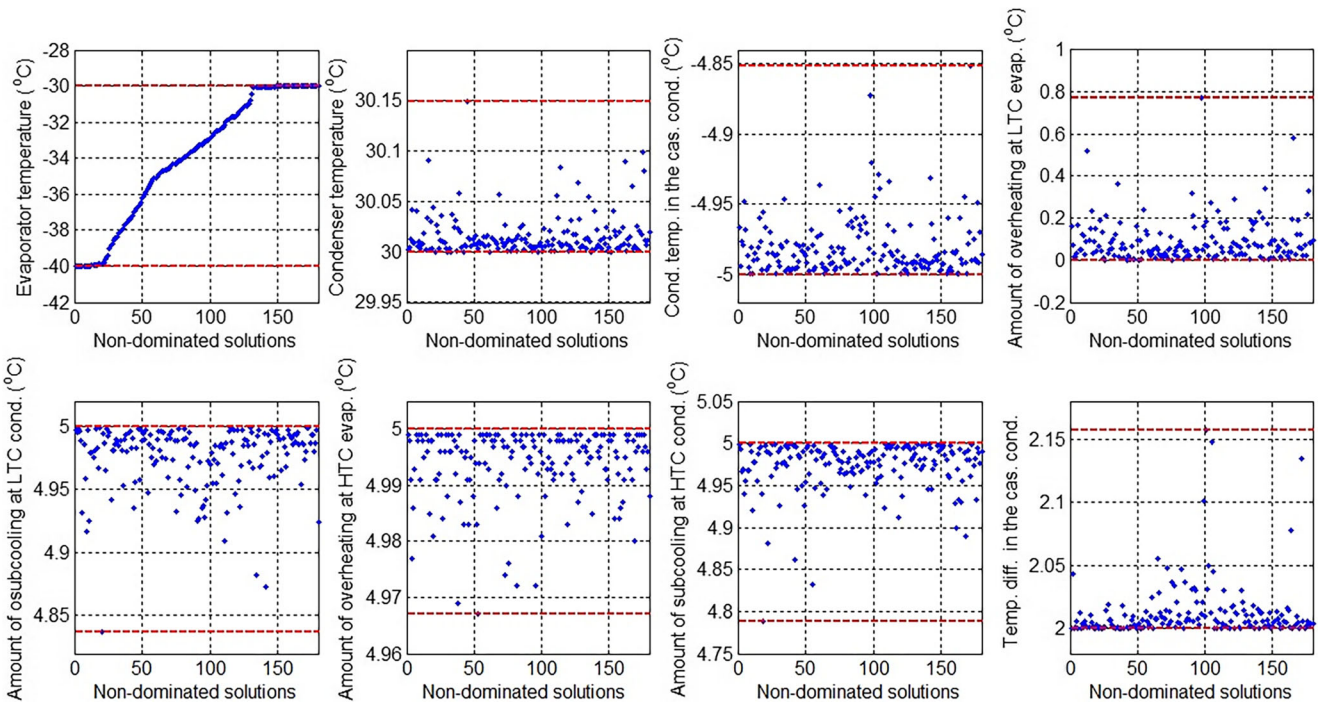

Fig. 7 Distribution of the design parameters along the Pareto frontier

Table 8 reports the optimal system parameters obtained for single and multi objective design purposes for R744/R1234yf cascade refrigeration cycle. As mentioned before, there are many research papers in the literature on the application R1234yf to refrigeration systems and experimental and theoretical studies on its possible replacement for R134a. Therefore, a comprehensive comparative performance analysis between these two refrigerants is another major issue that should be elaborately investigated in this study. When single objective optimization is performed, similar tendencies are observed for the design variables of R744/R1234 and R744/R134a refrigeration cycles. Overall COP of R744/R134a cascade cycle is lower than that of R744/R1234yf cycle for both optimization cases. The amount of required compressor work for HTC and LTC plays an important role for this difference. LTC compressor work rate obtained for each cascade cycle is quite similar, however HTC compressor work of R744/R1234yf cycle is 23.19% lower that of R744/R134a cycle when total annual cost of the system is minimized and HTC compressor work is 33.58% lower than that of R744/R134a cycle when second law efficiency is maximized. These corresponding decreases lead to an overall incease in COP rates for R744/R1234yf refrigeration cycle, which is increased by 9.95% when total annual cots of the system is optimized and increased by 19.29% when second law efficiency is optimized. It is also seen that minimum total annual cost of the R744/R1234yf cascade cycle is 6.71% lower than that of R744/R134a cycle while maximum second law efficiency of the R744/R1234yf cascade cycle is 21.25% higher than that of R744/R134a cascade cycle. Figure 8 shows the the non-dominated Pareto optimal solutions obtained for multi objective design optimization of R744/R1234yf cascade

Table 8 Single and multi objective optimization results of R744/R1234yf cascade refrigeration cycle

	Minimum total annual cost	Maximum second law efficiency	Multiobjective optimization
Evaporator temperature (°C)	−39.999	−30.001	−39.981
Overheat temperature at the bottom cycle (°C)	0.015	0.062	0.035
Amount of subcooling at the bottom cycle (°C)	4.972	4.999	4.985
Temperature difference in the cascade condenser (°C)	7.066	2.000	7.042
Condensing temperature of R744 in the cascade condenser (°C)	−4.999	−4.982	−4.993
Condenser temperature (°C)	30.000	30.939	30.014
Amount of overheat at the top cycle (°C)	4.965	4.992	4.986
Amount of subcooling at the bottom cycle (°C)	4.964	4.978	4.999
System outputs			
Mass flow rate of R1234yf (kg/s)	0.422	0.371	0.420
Mass flow rate of R744 (kg/s)	0.210	0.181	0.209
Total heat exchange area of the evaporator (m^2)	61.013	181.810	61.123
Total heat exchange area of the cascade condenser (m^2)	12.694	82.384	12.752
Total heat exchange area of the condenser (m^2)	5.824	3.961	5.811
Required compressor power for the bottom cycle (kW)	15.062	9.002	15.050
Required compressor power for the top cycle (kW)	14.074	10.865	14.048
Overall COP (−)	1.503	2.208	1.504
Component cost			
Cost of the bottom cycle compressor ($)	35,404.076	27,939.701	35,390.367
Cost of the top cycle compressor ($)	32,482.458	28,837.358	32,454.057
Cost of the evaporator ($)	55,679.363	144,754.254	55,765.964
Cost of the condenser ($)	7714.294	5662.437	7700.655
Cost of the cascade condenser ($)	13,413.891	47,849.914	13,456.163
Total cost of the system components ($)	144,694.085	255,043.666	144,767.208
Problem objectives			
Total annual cost ($)	37,829.411	51,807.055	37,384.315
Second law efficiency (−)	0.45128	0.55385	0.45171

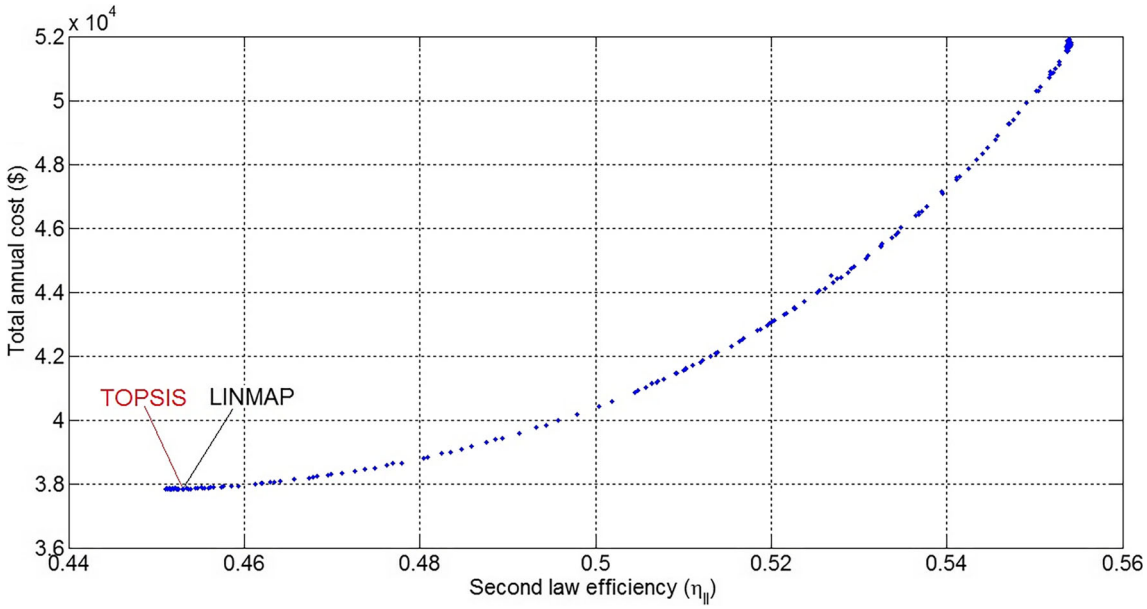

Fig. 8 Pareto frontier for optimum design of R744/R1234yf cascade refrigeration cycle

refrigeration cycle. According to the best optimal results selected by LINMAP and TOPSIS decision makers, optimal values of the design objectives are 37,384.315 $ for the total annual cost and 0.45171 for the second law efficiency. Figure 9 shows the variatonal changes of the design variables throughout the Pareto curve built for the optimal design of R744/R1234yf cascade refrigeration cycle. It is clearly seen that decision variables of evaporation temperature and temperature difference in the cascade condenser vary between the upper and lower limits along the frontier while other design variables are accumulated at upper or lower bounds of the search domain. Tendencies of these two design variables create a trade- off in the Pareto domain, which entails an increase in total annual cost rates by 36.95% and increase in second law efficiency values by 22.73%. Figure 10 visualizes the T-s diagram representation of three mentioned cascade

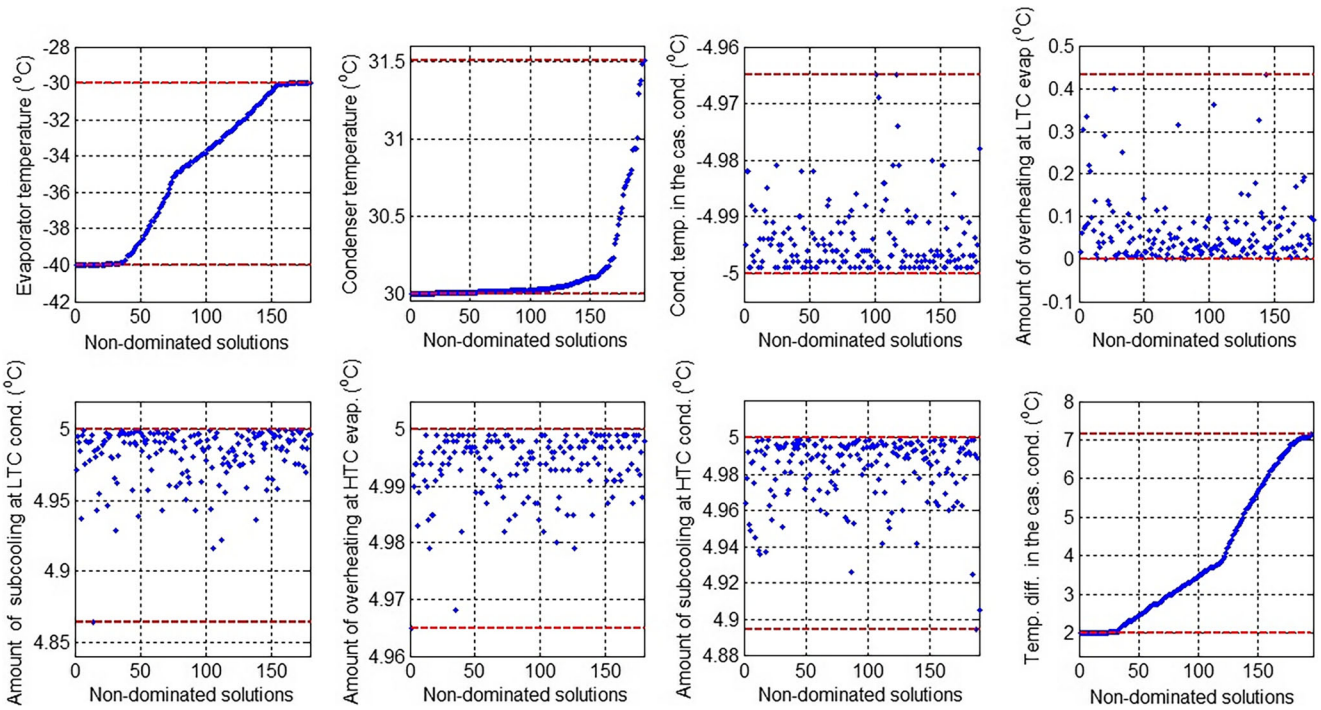

Fig. 9 Variational distribution of the system design parameters across the Pareto curve

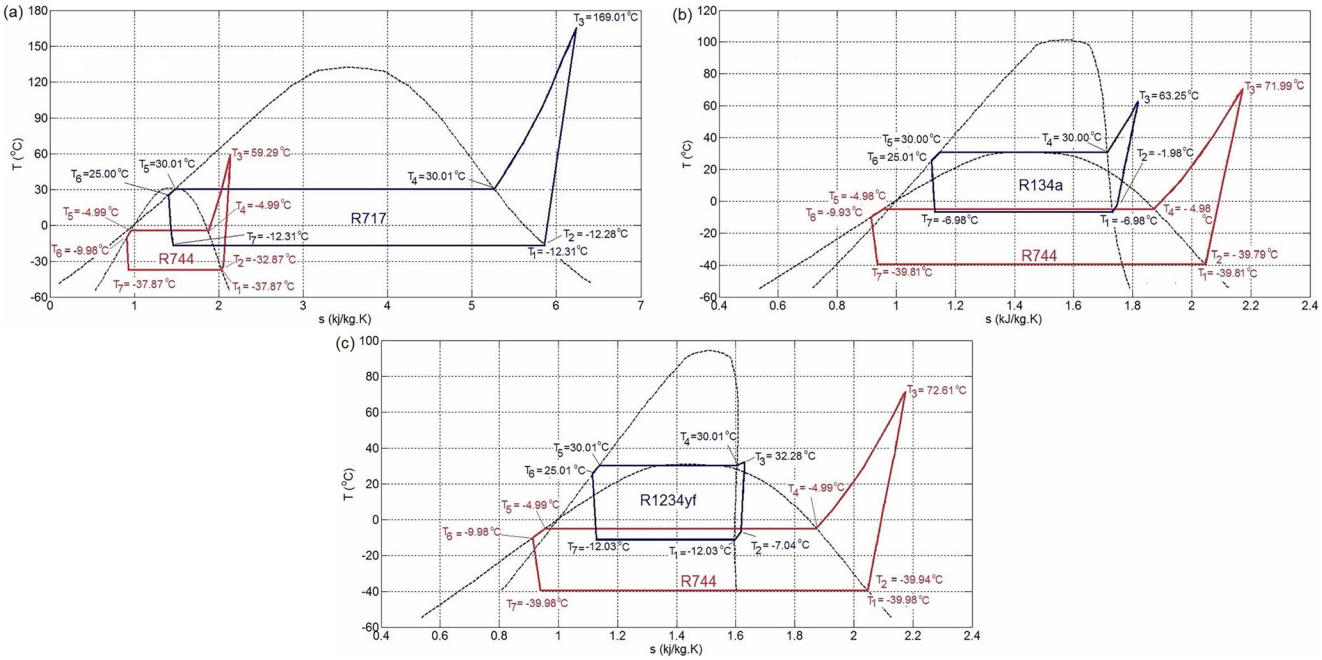

Fig. 10 T-s diagram of the **a** R744/R717, **b** R744/R134a, and **c** R744/R1234yf cascade refrigeration cycles operated under optimal conditions

refrigeration cycles while operating at the optimal conditions obtained from TOPSIS and LINMAP methods. Table 9 tabulates the thermodynamic properties of the critical state points of the mentioned cycles shown in Fig. 10.

Sensitivity analysis is performed to observe the effects of the variations of the system parameters on design objectives. The optimal values of the decision variables obtained by TOPSIS and LINMAP theorems are considered in evaluating the influences of design parameters over problem objectives. Values of remaining parameters stays constant during evaluations. Figure 11 shows the effects of the design variables of evaporator and condenser temperature, temperature difference in cascade condenser, and R744 condensing temperature over the cycle equipment cost. It is seen that increase in condenser temperature leads to an increase in HTC compressor cost for each cycle configuration. However, this increase induces a reduction in condenser cost. A marked increase is observed in LTC compressor cost for each cycle with increasing R744 condensing temperatures. On the other hand, HTC compressor cost considerably goes down as a result of this increase, particularly for R744/R134a and R744/R1234yf refrigeration cycles. There also occurs an increase in cascade condenser cost while remarkable decrease is evident for evaporator cost for each cycle configuration. It is seen that increasing evaporator temperatures entail an enhancement in the cost rates of each equipment of each cycle configuration. As temperature difference in the cascade condenser increases, a huge amount of reduction in the cost rates of the cascade condenser of R744/R717 and R744/R1234yf cycles occurs while this reduction in cost rates is relatively lower for the cascade condenser of R744/R134a cycle. In addition, HTC compressor cost of each cycle is slighly increased with this increasing temperature difference. Figure 12 shows the influences of the overheating and subcooling temperatures on the equipment cost rates of each cycle configuration. It is observed from the figure that any increase in the overheat and subcooling temperatures has little influence over equipment cost rates.

Figure 13 visualizes the effects of design variables over the second law efficiency values of each cycle configuration. Second law efficiency considerably increases with increasing evaporator temperatures while dramatical decreases are observed for this objective as R744 condensing temperature increases. A slight decrease is seen in second law efficiency of R744/R134a cycle with increasing condenser temperatures. As overheat amount increases at the bottom cycle side, second law efficiency of the R744/R717 cascade cycle increases while this parameter is in decreasing trend for other compared cycles. A fair increase is seen for second law efficiency values with increasing overheating and subccoling temperatures at the top and bottom side of each refrigeration cycle. Increasing overheat temperatures at the the top side of the cycle causes a significant increase in second law efficiencies of R744/R134a and R744/R1234yf refrigeration cycles, however induce a

Table 9 Thermodynamic properties of the state points of three cascade refrigeration cycles shown in Fig. 10

		Temp. (°C)	Pressure (kPa)	Enthalpy (kJ/kg)	Entropy (kJ/kg.K)
R744	State 1	−37.87	1085.466	435.743	2.037
	State 2	−32.87	1085.466	440.941	2.059
	State 3	59.29	3046.150	512.611	2.138
	State 4	−4.99	3046.150	433.378	1.872
	State 5	−4.99	3046.150	188.057	0.957
	State 6	−9.98	3046.150	176.310	0.915
	State 7	−37.87	1085.466	176.310	0.935
R717	State 1	−12.31	264.409	1447.819	5.789
	State 2	−12.28	264.409	1392.838	5.789
	State 3	169.01	1167.200	1849.458	6.256
	State 4	30.01	1167.200	1486.170	5.263
	State 5	30.01	1167.200	341.762	1.488
	State 6	25.00	1167.200	317.741	1.408
	State 7	−12.31	264.409	317.741	1.457
R744	State 1	−39.81	1004.795	435.321	2.048
	State 2	−39.79	1004.795	435.607	2.049
	State 3	71.99	3051.751	526.655	2.180
	State 4	−4.98	3051.751	433.350	1.872
	State 5	−4.98	3051.751	188.215	0.958
	State 6	−9.93	3051.751	176.466	0.916
	State 7	−39.81	1080.812	176.466	0.936
R134a	State 1	−6.98	225.640	394.501	1.731
	State 2	−1.98	225.640	397.462	1.747
	State 3	63.25	770.399	448.646	1.820
	State 4	30.00	770.399	414.825	1.714
	State 5	30.00	770.399	241.735	1.143
	State 6	25.01	770.399	234.588	1.119
	State 7	−6.98	225.640	234.588	1.130
R744	State 1	−39.98	1005.165	435.323	2.048
	State 2	−39.94	1005.165	435.363	2.048
	State 3	72.61	3046.401	526.006	2.178
	State 4	−4.99	3046.401	433.377	1.872
	State 5	−4.99	3046.401	188.066	0.957
	State 6	−9.98	3046.401	176.323	0.915
	State 7	−39.98	1006.498	176.323	0.938
R1234yf	State 1	−12.03	204.466	355.272	1.596
	State 2	−7.04	204.466	361.101	1.618
	State 3	32.28	780.629	392.022	1.631
	State 4	30.01	780.629	381.675	1.605
	State 5	30.01	780.629	240.322	1.138
	State 6	25.01	780.629	233.306	1.115
	State 7	−12.03	204.466	233.306	1.129

slight reduction in that of R744/R717 refrigeration cycle. Increasing temperature differences in the cascade condenser has a negative effect on second law efficiency values since notable decreases are seen in second law efficiency rates as this design parameter varies from its lower to upper bounds. Figure 14 illustrates and investigates the sensitivity of the Pareto frontier built for each compared refrigeration cycle as a function of changing cooling load values in order to the observe the effects of the amount of cooling rates on dual problem

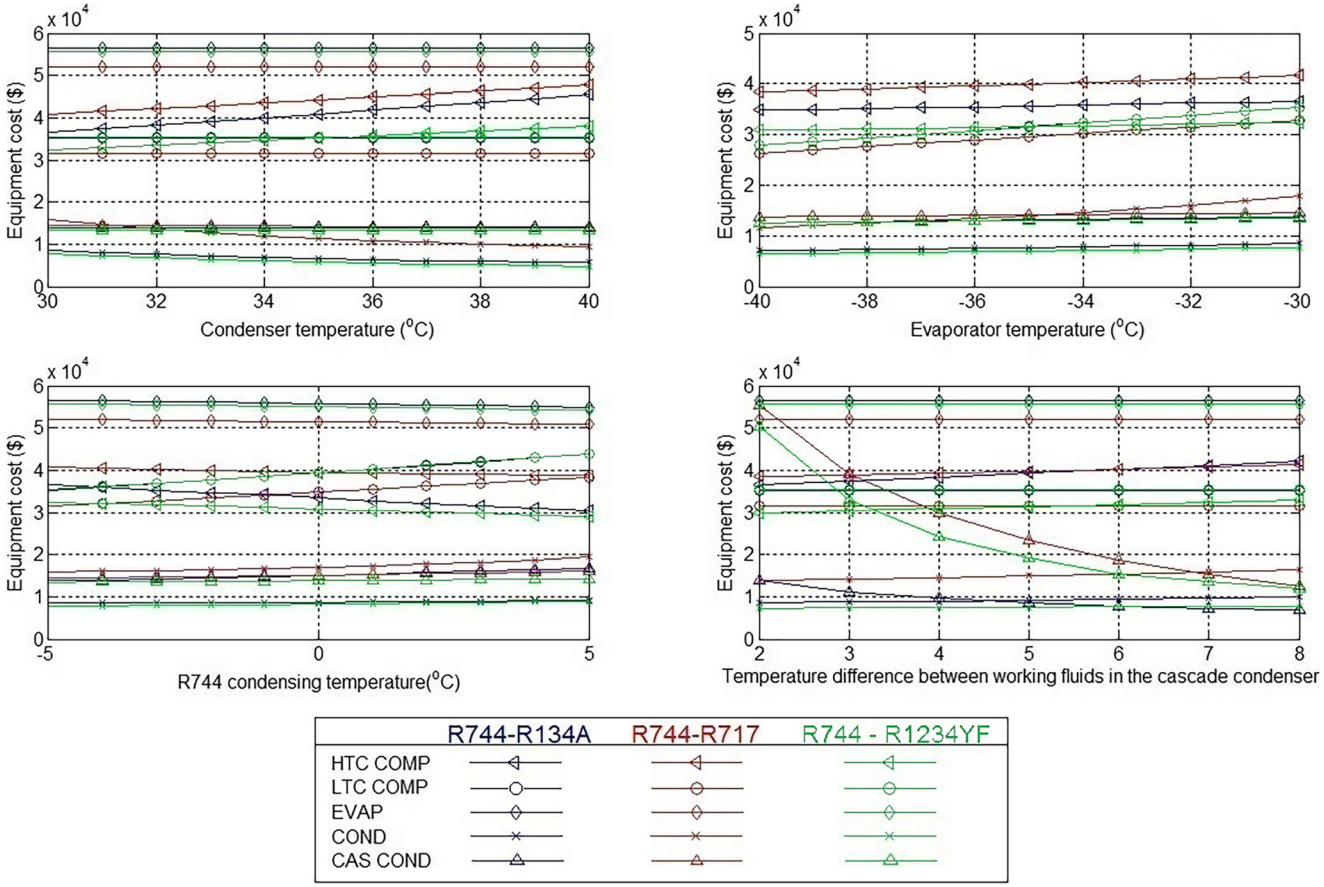

Fig. 11 Variational changes of the equipment cost rates with respect to the design variables

objective. As expected and understood from the figure, Pareto curves moves upward and slightly rightward with increasing cooling load values.

6 Conclusion

This theoretical research study aims to carry out performance analysis of R744/R717, R744/R134a, and R744/R1234yf in terms of energetic, exergetic and economic points of view. The results of the mathematical model used to design cascade refrigeration cycle are validated againts the outcomes of a previous literature study in order to investigate the accuracy of the proposed thermodynamical model. Artificial Cooperative Search metaheuristic algorithm is applied to obtain optimal design points of each refrigeration cycle mentioned in this study. Second law efficiency and total annual cost of the cascade refrigeration cycle are considered as design objectives to be optimized individually and simultaneously. Single objective optimization results reveal that maximum second law efficiency obtained for R744/R1234yf refrigeration cycle is higher than those of the compared refrigeration cycles. Optimization results reveal again the superiority of R744/R1234yf refrigeration cycle over other compared cycles with respect to the attained minimum annual total cost rates. Multi objective optimization is performed for each cycle to obtain a set of non-dominated solutions those resulted from the trade-off between conflicting objectives. After non-dimensionalization of each pareto solution the frontier, TOPSIS and LINMAP decision making theorems are applied to choose the best results among the alternative solutions on the curve. According to the distribution of decision variables along the pareto frontier, it can be concluded that condenser temperature and temperature difference in the cascade condenser are two decisive design parameters those creating a trade-off between problem objectives. It is seen that best results obtained by TOPSIS and LINMAP methods are tended towards minimum total annual cost and second law efficiency for each cycle configuration. Parametric sensitivity analysis has been performed to scrutinize the effects of varying design variables on problem objectives. It is observed that subcooling and overheating temperatures at the bottom and top sides have a negligible influence on cycle equipment cost. Another conclusion resulted from sensitivity analysis is that second law efficiency of each cascade cycle is markedly affected by the variations of evaporator temperature, R744 condensing

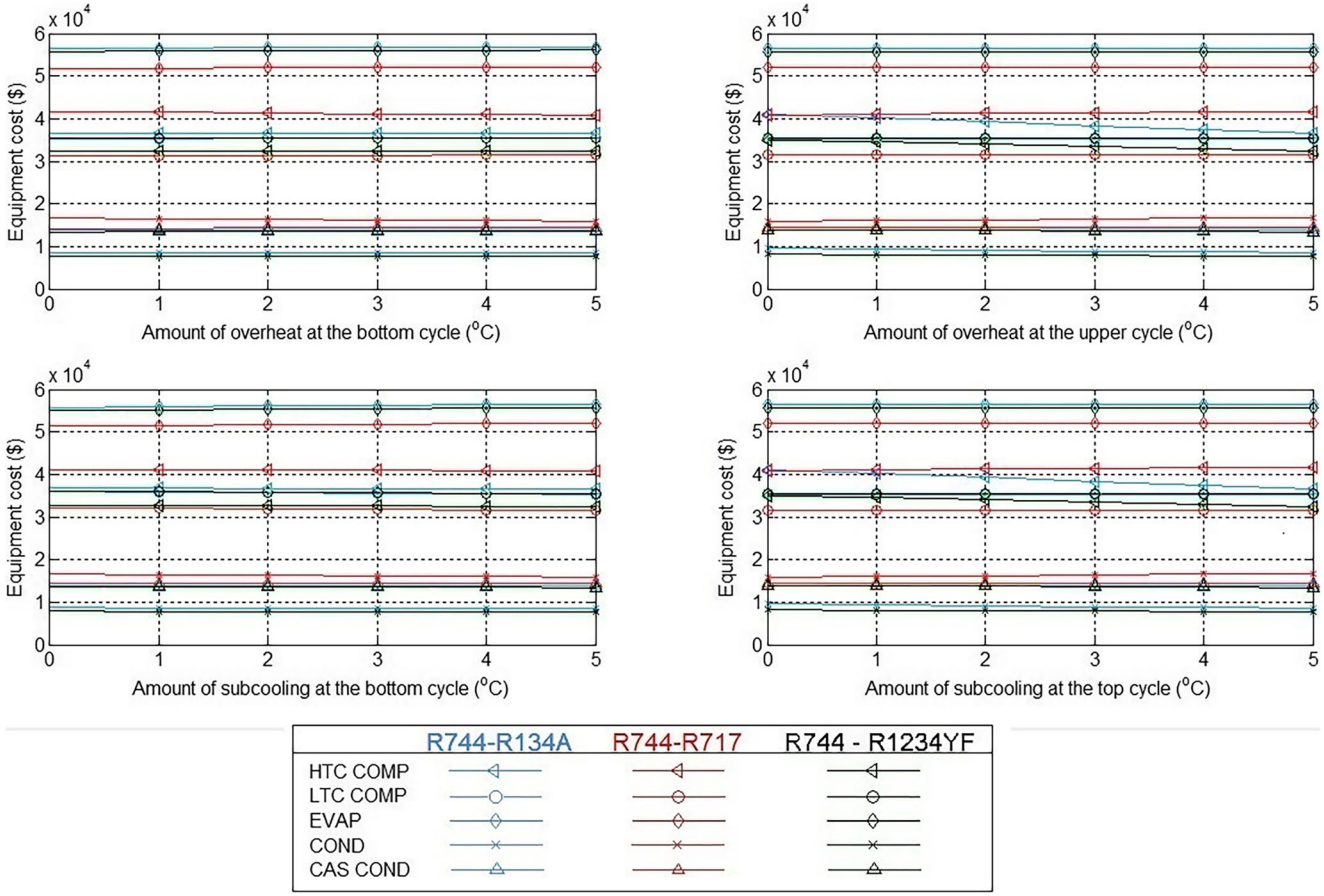

Fig. 12 Effects of subcooling and overheating temperatures on the equipment cost rates of each cycle configuration

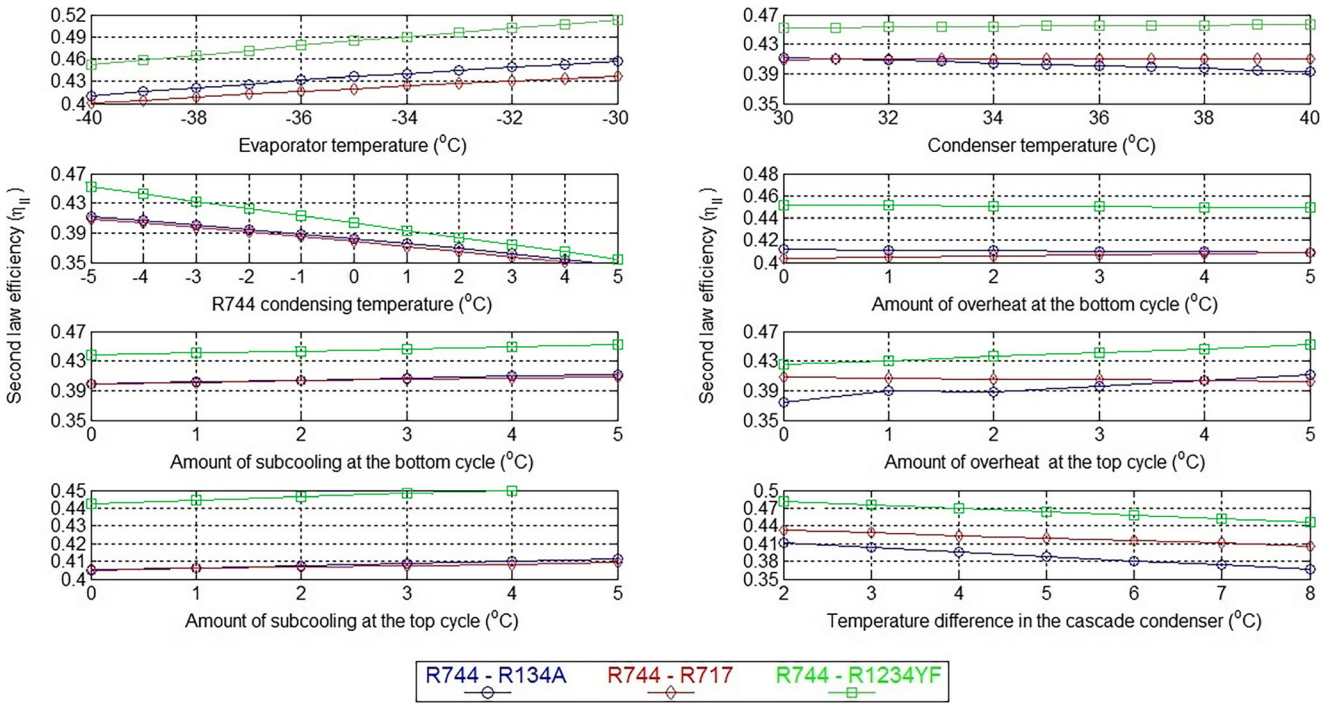

Fig. 13 Variations of second law efficiency with regard to increasing values of decision variables

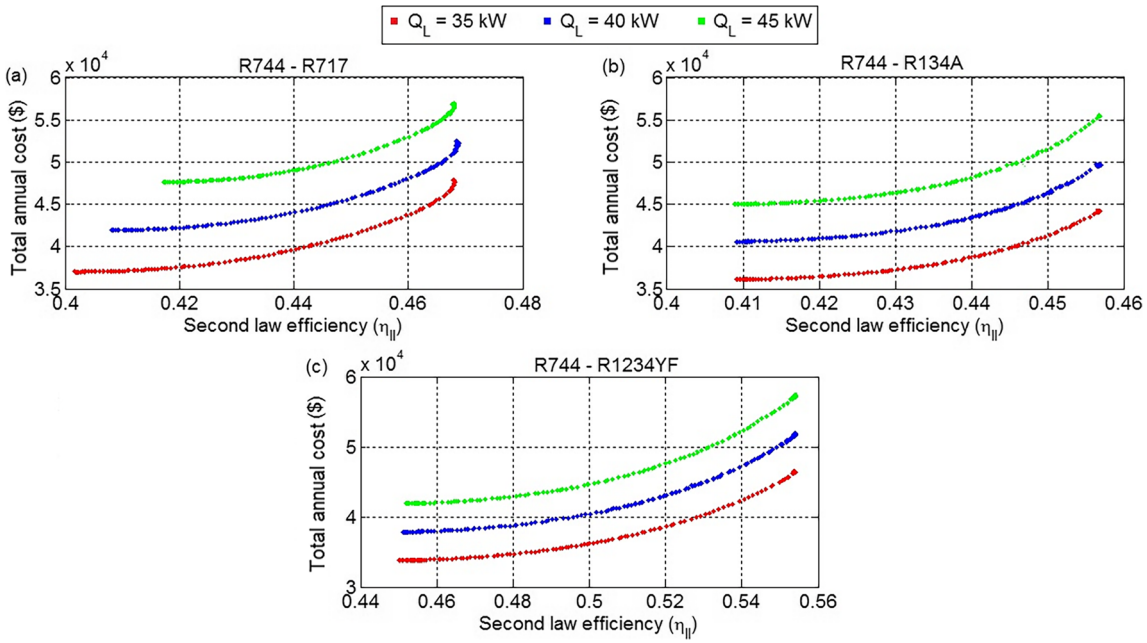

Fig. 14 Variations of the optimal values of the dual objectives with respect to increasing cooling load rates

temperature, and temperature difference in the cascade condenser. A detailed sensitivity analysis is also carried out to investigate the influences of cooling load rates over the obtained Pareto front. Optimal values given in these study can be utilized as a reference point for end users while modelling and designing a real cascade refrigeration cycle system.

Compliance with ethical standards

Conflict of interest On behalf of all authors, the corresponding author states that there is no conflict of interest.

Ethical approval This article does not contain any studies with human participants or animals performed by any of the authors.

Informed consent Informed consent was obtained from all individual participants included in the study.

Publisher's Note Springer Nature remains neutral with regard to jurisdictional claims in published maps and institutional affiliations.

References

1. Kilicarslan A, Hosoz M (2010) Energy and irreversibility analysis of a cascade refrigeration for various refrigeration couples. Energ Convers Manage 51:2947–2954
2. Bansal P (2012) A review – status of CO_2 as a low temperature refrigerant: Fundamentals and R&D opportunities. Appl Therm Eng 41:18–29
3. Lee T-S, Liu C-H, Chen T-W (2006) Thermodynamic analysis of optimal condensing temperature of cascade condenser in CO_2/NH_3 cascade refrigeration systems. Int J Refrig 29:1100–1108
4. Lorentzen G, Petterson J (1993) A new efficient and environmentally benign system for car air conditioning. Int J Refrig 16:4–12
5. Lorentzen G (1995) The uses of natural refrigeant a complete solution tothe CFC/HCFC predicament. Int J Refrig 18:190–197
6. Dopazo JA, Fernandez-Seara J, Sieres J, Uhia FJ (2009) Theoretical analysis of a $CO_2 – NH_3$ cascade refrigeration system for cooling applications at low temperatures. Appl Therm Eng 29:1577–1583
7. Dokandari DA, Hagh AS, Mahmoudi SMS (2014) Thermodynamic investigation and optimization of novel ejector-expansion CO_2/NH_3 cascade refrigeration cycles (novel CO_2/NH_3 cycle). Int J Refrig 46:26–36
8. Ozgur AE, Kabul A, Kizilkan O (2014) Exergy analysis of refrigeration systems using an alternative refrigerant (HFO – 1234yf) to R134a. Int J Low-Carbon Tech 9:56–62
9. SAE International (2008) Industry evaluation of low global warming potential refrigerant HFO 1234yf, SAE Report CRP 1234. Accessed 28 August 2017
10. Park KJ, Jung D (2010) Nucleate boiling heat transfer coefficicentof R1234yf on plain and low fin surfaces. Int J Refrig 33:553–557
11. Tanaka K, Higashi Y (2010) Thermodynamic properties of HFO-1234yf (2,3,3,3-tetra-fluoropropene). Int J Refrig 33:474–479
12. Lee Y, Jung D (2012) A brief performance comparison of R1234yf and R134a in a bench tester for automobile applications. Appl Therm Eng 35:240–242
13. Yataganbaba A, Kilicarslan A, Kurtbas I (2015) Exergy analysis of R1234yf and R1234ze as R34a replacements in a two evaporator vapour compression refrigeration system. Int J Refrig 60:26–37
14. Navarro-Esbri J, Miranda-Mendoza JM, Mota-Babiloni A, Barragan-Cervera A, Belman-Flores JM (2013) Experimental analysis of R1234yf as a drop-in replacement for R134a in a vapor compression system. Int J Refrig 36:870–880
15. Zilio C, Brown JS, Schiochet G, Cavallini A (2011) The refrigerant R1234yf in air conditioning systems. Energy 36:6110–6120
16. Aminyavari M, Najafi B, Shirazi A, Rinaldi F (2014) Exergetic, economic and environmental (3E) analyses, and multi-objective optimization of a CO_2/NH_3 cascade refrigeration system. Appl Therm Eng 65:42–50
17. Rezayan O, Behbahaninia A (2011) Thermoeconomic optimization and exergy analysis of CO_2/NH_3 cascade refrigeration systems. Energy 36:888–895

18. Civicioglu A (2013) Artificial cooperative search algorithm for numerical optimization problems. Inf Sci 229:58–76
19. Bell IH, Wronski J, Quoilin S, Lemort V (2014) Pure and Psudo-pure Fluid Thermophysical Property Evaluation and the Open-Source Thermophysical Propoerty Library CoolProp. Ind Eng Chem Res 53:2468–2508
20. Petter N, Filippo D, Havard R, Arne B (2004) Measurements and experience on semi-hermetic CO_2 compressor. Fifth International Conference on Compressors and Coolants, IIR, Slovak Republic
21. Stoecker WF (1998) Industrial refrigeration handbook. McGraw Hill, New York
22. Mallick AR (2014) Practical boiler operation engineering and power plant. PHI Learning, New Delhi
23. Kraus AD, Aziz A, Welty J (2001) Extended surface heat transfer. John Wiley & Sons, Hoboken
24. Gungor KE, Winterton RHS (1987) A General Correlation for Flow Boiling in Tubes and Annuli. Int J Heat Mass Transf 29(3):351–358
25. Fang X (2013) A new correlation of flow boiling heat transfer coefficients for carbon dioxide. Int J Heat Mass Transf 64:802–807
26. Fang X (2013) A new correlation of flow boiling heat transfer coefficients based on R134a data. Int J Heat Mass Transf 66:279–283
27. Cavallini A, Del Col D, Doretti L, Matkovic M, Rosetto L, Zilio C, Censi G (2006) Condensation in Horizontal Smooth Tubes: A New Heat Transfer Model for Heat Exchanger Design. Heat Transf Eng 27:31–38
28. Fronk BM, Garimella S (2016) Condensation of ammonia and high-temperaturglide zeotropic ammonia/water mixtures in minichannels – Part II: Heat transfer models. Int J Heat Mass Transf 101:1357–1373
29. Kern DQ (1958) Mathematical development of loading in horizontal condensers. AICHE J 4:157–160
30. Wang H, Fang X (2016) Evaluation analysis of correlations of flow boiling heat transfer coefficients applied to ammonia. Heat Transfer Eng 37:32–44
31. Shah MM (2009) An Improved and Extended General Correlation Heat Transfer During Condensation in Plain Tubes. HVAC&R Res 15:889–913
32. Smith R (2005) Chemical Process: Design and Integration. John Wiley & Sons, New York
33. Qu S, Goh M, Chan FTS (2011) Quasi-Newton methods for solving multi objective optimization. Oper Res Lett 39:397–399
34. Datta S, Ghosh A, Sanyal K, Das S (2017) A Radial Boundary Intersection aided interior point method for multi objective optimization. Inf Sci 377:1–16
35. Ehrgott M, Puerto J, Chia AMR (2007) Primal-Dual Simplex Method for Multiobjective Linear Programming. J Optim Theory Appl 134:483–497
36. Zilinsaks A, Zhigljavsky A (2016) Branch and probability bound methods in multi-objective optimization. Optim Lett 10:341–353
37. Holland JH (1975) Adaptation in natural and artificial systems. MIT Press, Cambridge
38. Dorigo M, Stützle T (2004) Ant colony optimization. MIT Press, Cambridge
39. Geem ZW, Kim JH, Loganathan GV (2001) A new heuristic optimization algorithm: harmony search. Simulation 76:60–68
40. Sanchez-Orgaz S, Pedemonte M, Ezzatti P, Curto-Risso PL, Medina A, Calvo Hernandez A (2015) Multi objective optimization of a multi-step solar-driven Braydon plant. Energ Convers Manage 99:346–358
41. Mwesigye A, Bello-Ochende T, Meyer JP (2015) Multi-objective and thermodynamic optimization of a parabolix trough reciever with perforated plate inserts. Appl Therm Eng 77:42–56
42. Yao E, Wang H, Wang L, Xi G, Marechal F (2017) Multiobjective optimization and exergoeconomic analysis of a combined cooling, heating and power based compressed air energy storage system. Energ Convers Manage 138:199–209
43. Luo Z, Sultan U, Ni M, Peng H, Bingwei S, Xiao G (2016) Multi objective optimization for GPU3 Stirling engine by combining multi - objective algorithms. Renew Energy 94:114–125
44. Baserati SM, Ataskari K, Jamali A, Hajiloo A, Nariman-zadeh N (2010) Multi objective thermodynamic optimization of combined Brayton and inverse Brayton cycles using genetic algorithms. Energ Convers Manage 51:212–217
45. Arora R, Kaushik SC, Kumar R (2016) Multi-objective thermodynamic optimization of solar parabolic dish stirling heat engine with regenerative losses using NSGA-II and decision making. Appl Sol Energ 52:295–304
46. Kaboli SHA, Selveraj J, Rahim NA (2016) Long term electric energy consumption forecasting via artificial cooperative search algorithm. Energy 115:857–871
47. Kumar SR, Ganapathy S (2014) Artificial Cooperative Search Algorithm based Load Frequency Control of Interconnected Power Systems with AC-DC Tie-lines. Int J Eng Tech 6:701–706
48. Rajamanickam CS, Karthikeyan CP, Samuel AA (2016) Influence of Refrigerant (R134a/R1234yf) Properties on Cooling Performance of an Automobile Hvac. Int J Appl Eng Res 11: 3703–3707
49. Wei X, Fang X, Shi R (2012) A Comparative Study of Heat Transfer Coefficients for Film Condensation. Eng Sci Tech 3:1–9
50. Arslan G, Eskin N (2015) Heat Transfer Characteristics for Condensation of R134a in a Vertical Smooth Tube. Exp Heat Transfer 28:430–445
51. Agarwal R, Hrnjak P (2015) Condensation in two phase and desuperheating zone for R1234ze(E), R134a and R22 in horizontal smooth tubes. Int J Refrig 50:172–183
52. Fronk BM, Garimella S (2016) Condensation of ammonia and high-temperature-glide zeotropic ammonia/water mixtures in minichannels – Part II: Heat transfer models. Int J Heat Mass Transf 101:1357–1373